Michigan State University

National Superconducting Cyclotron Laboratory

MULTIFRAGMENT DISINTEGRATION OF THE $^{129}Xe + ^{197}Au$ SYSTEM AT E/A = 50 MeV

D.R. BOWMAN, G.F. PEASLEE, R.T. de SOUZA, N. CARLIN, C.K. GELBKE, W.G. GONG, Y.D. KIM, M.A. LISA, W.G. LYNCH, L. PHAIR, M.B. TSANG, C. WILLIAMS, N. COLONNA, K. HANOLD, M.A. McMAHAN, G.J. WOZNIAK, L.G. MORETTO, and W.A. FRIEDMAN

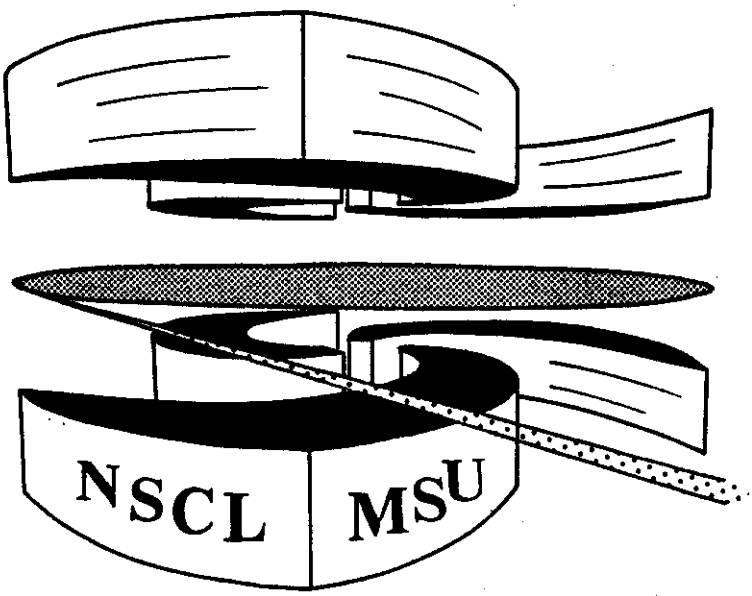

MSUCL-779 **MAY 1991**

MSUCL-779
May, 1991

"Multifragment disintegration of the $^{129}Xe+^{197}Au$ system at E/A=50 MeV"

D.P. Bowman, G.F. Peaslee, B.T. de Sousa, N. Carlin,† C.K. Gelbke,
W.G. Gong, Y.D. Kim, N.A. Lisa, W.G. Lynch, L. Phair, M.B. Tsang, C. Williams
National Superconducting Cyclotron Laboratory
and Department of Physics and Astronomy
Michigan State University, East Lansing, MI. 46024

N. Colonna, K. Hanold, N.A. McMahan, G.J. Wozniak, L.G. Moretto
Nuclear Science Division and Accelerator and Fusion Research Division
Lawrence Berkeley Laboratory, Berkeley, CA. 94720

W.A. Friedman
Department of Physics, University of Wisconsin, Madison, WI. 53706

Abstract

Multifragment disintegrations following $^{129}Xe+^{197}Au$ collisions at E/A=50 MeV have been measured with a multidetector system covering 88% of 46 in solid angle. The average number of intermediate mass fragments (Z=3-20) increases strongly as a function of charged particle multiplicity and reaches values slightly larger than six for the most violent collisions. Comparisons to statistical model calculations show that such multifragment final states are consistent with the breakup of sources at densities significantly less than normal nuclear density.

PACS index: 25.70.-s, 25.70.Gh, 25.70.Np

The disintegration of highly excited nuclear systems into nucleons and bound clusters is predicted both by statistical [1-5] and dynamical theories [6-8]. Multifragment decays are of particular interest since they may represent a new mode of nuclear disassembly. Several possible mechanisms may be responsible for this process. The system might, for example, evolve into strongly oblate or prolate shapes where Rayleigh instabilities could lead to multifragmentation [9]. The expansion of an initially hot and possibly compressed system can lead to high temperatures and low densities in which density fluctuations can cause instabilities or a phase change [5,10-12]. Statistical emission mechanisms for complex fragments may be enhanced under the extreme conditions reached by the system. Some of these processes are governed by the equation-of-state of hot dilute nuclear matter.

Recent calculations [5] of the statistical decay of an expanding nuclear system predict a dramatic increase in fragment multiplicity when the thermal pressure becomes sufficient to cause an expansion to 0.4 times normal nuclear density. This prediction is largely untested by experimental data since very few experiments have been performed with sufficient phase space coverage to allow for the extraction of intermediate mass fragment multiplicities [13-18]. In order to test various fragment production models, we have measured charged particle and intermediate mass fragment (IMF, Z=3-20) multiplicities for the $^{129}Xe+^{197}Au$ reaction at E_{cm}=3.9 GeV, using a low-threshold 4π charged-particle detector [19].

A ^{129}Xe beam with intensity of 10^7 particles/s and energy of E/A=49.8 MeV, extracted from the K1200 cyclotron of the NSCL at Michigan State University,

impinged upon a 1.05 mg/cm^2 gold target. Reaction products were detected with 171 elements of the MSU Miniball phoswich detector array [19] which covered polar angles of $16^\circ \leq \theta \leq 160^\circ$, corresponding to approximately 87% of 4π. More forward angles were covered by a hodoscope consisting of 16 telescopes, each containing two position-sensitive solid-state detectors (300 μm and 5 mm thick) and a 7.6 cm thick plastic scintillator [20]. This forward hodoscope covered approximately 64% of the solid angle at $2^\circ \leq \theta \leq 16^\circ$ or 1.2% of 4π. Fragments were identified by element for Z≈1-20 in the Miniball with representative detection thresholds of 2, 3, and 4 MeV/nucleon for Z=3, 10, and 18 fragments, respectively. Element identification was achieved for Z=1-54 for particles punching through the 300 μm silicon ΔE-elements of the forward hodoscope; representative detection thresholds were 6, 13, 21, and 27 MeV/nucleon for Z=2, 8, 20, and 54 fragments, respectively.

Measured multiplicity distributions (not corrected for detector acceptance) are shown in Fig. 1. The upper panel shows the probability distribution for N_C, the detected charged particle multiplicity. We include, for orientation, rough estimates of the impact parameter, following ref. [21], and of the excitation energy of a fully thermalized nucleus consisting of 300 nucleons using the statistical model of ref. [5]. The lower panel shows probability distributions of the number of detected intermediate mass fragments ($3 \leq Z \leq 20$), N_{IMF}, for various gates on charged particle multiplicity. The average number of detected intermediate mass fragments increases with charged particle multiplicity, reaching a value of $\langle N_{IMF} \rangle = 6.0$ for the most central gate, $N_C \geq 33$. This is the largest average fragment multiplicity so far observed in any nuclear

collision. (This value is reduced to $\langle N'_{IMF}\rangle$=4.7 when Z=3 fragments are excluded.) Collisions are observed with up to 14 intermediate mass fragments in the final state.

In Fig. 2, we present Z_{sum}, the total charge of all identified particles detected at $5.6^\circ \leq \theta \leq 160^\circ$ for different gates on charged particle multiplicity [22]. For the highest multiplicity gate, $N_C \geq 33$, the average value of Z_{sum}=84 corresponds to 63% of the total charge of the composite system, and a number of events were observed with a detected charge larger than 90% of the total charge. In these latter collisions virtually no fragments with Z>20 were recorded. Our measurements are qualitatively consistent with the observation [23] of a nearly complete disintegration of the composite system into light particles and intermediate mass fragments for central $^{208}Pb+^{197}Au$ collisions at $E_{cm} \approx 3$ GeV.

We have performed calculations to test whether comparable multiplicities are predicted by the microscopic quasi-particle dynamics (QDP) model of ref. [8]. Most calculations were followed out to times of t=300 fm/c when fast non-equilibrium emission has ceased [24]. In collisions leading to a total multiplicity of 36-45, these calculations predict average multiplicities less than one for fragments with $3 \leq Z \leq 20$ and, in addition, the formation of a single heavy residue. These predicted IMF multiplicities are much smaller than those observed experimentally. The predicted residual nuclei are still highly excited ($E^*_{tot} \approx 1.5$ GeV) and a few exploratory calculations were performed to much longer times, t=3000 fm/c, to investigate whether the calculations would predict the emission of additional fragments. Instead, the calculated number

of intermediate mass fragments decreased slightly due to particle decays of fragments formed at the earlier stages of the reaction.

We also explored the multiplicities of fragments predicted by statistical model calculations of compound nucleus decay. Since detailed predictions of statistical model calculations depend on the initial mass, charge, and excitation energy of the excited nucleus, calculations were performed for a variety of initial conditions. Even though the excitation energies used in some of these calculations may exceed the region of applicability of these models, such calculations may, nevertheless, provide useful information about the population of final states due to phase space considerations and may, therefore, provide instructive comparisons to dynamical treatments.

The open circles and crosses in Fig. 3 provide the multiplicities predicted by the statistical model code GEMINI [25] for the decay of highly excited and equilibrated Xe and Au nuclei, respectively, with excitation energies of E*(Xe)=0.5, 1.0, 1.5, and 2.0 GeV and E*(Au)=1.0, 1.5, 2.0, and 2.5 GeV. In this code, all binary mass divisions from light particle evaporation to symmetric fission are considered, and sequential decays of particle unstable primary fragments are incorporated. For each calculation, a level density parameter of a=A/(8.5 MeV) was used and initial angular momenta of I(Xe)=87 $\hbar$ and I(Au)=80 $\hbar$ were assumed (these are the maximum angular momenta for which barriers exist for all decay channels). For large charged particle multiplicities, $N_C \gtrsim 30$, the calculated average fragment multiplicities, $\langle N_{IMF} \rangle \leq 2$, are much smaller than those observed experimentally (solid points). The calculations underpredict the observed large IMF multiplicities for a

broad range of scenarios considering the statistical decay of highly excited projectile-like and target-like fragments, including scenarios in which the available excitation energy is shared equally or in proportion to the masses of these fragments [26].

Comparably small fragment multiplicities are predicted by the statistical evaporation model of ref. [4]. The many different dashed curves in Fig. 3 depict the temperature dependence of multiplicities predicted for a variety of initial masses (A=275-326) and charge-to-mass ratios (Z/A=0.367-0.433). The results are qualitatively similar to the GEMINI calculations [25]; too few intermediate mass fragments are predicted for charged particle multiplicities greater than 30.

In the preceding statistical model calculations, the nuclei were constrained to remain at normal nuclear density by an implicit model assumption. Such a constraint could arise for nuclei characterized by an extremely stiff equation of state. Drastically different results are obtained for statistical model calculations [5] for a heated nucleus with a finite-nucleus compressibility coefficient K=144 MeV which is allowed to expand under the influence of thermal pressure. These calculations are shown by the solid curves for the same range of masses, charges and temperatures used in the calculations for the non-expanding systems [4]. Not only are significantly larger IMF multiplicities predicted, but the trend with increasing charged particle number is in reasonable agreement with the data. The calculations suggest that many of the fragments may be emitted from a system at reduced density. The solid curves represent heated systems which expand, without initial collective

kinetic energy, from normal density. As a consequence of compression prior to the decay process, the systems may possess a collective expansion energy as they pass through normal density. The model predicts even larger fragment multiplicities for non-zero collective expansion energies. For example, an initial expansion kinetic energy of about 50 MeV increases the predicted IMF multiplicities by roughly one unit.

To illustrate the possible influence of detection thresholds and incomplete solid angle coverage on the measured charged particle and IMF multiplicities, we have filtered representative theoretical results by the response of our experimental apparatus. In Fig. 3, the open diamonds represent the original model predictions and the star-shaped points show the corresponding values after taking the response of our experimental apparatus into account. Once the acceptance of our apparatus is taken into account (star shaped points), excellent agreement between the raw data (solid points) and the statistical calculations for expanding nuclear systems is obtained. Instrumental uncertainties do not affect our qualitative conclusions.

In summary, we have investigated collisions of $^{129}Xe+^{197}Au$ at E/A=50 MeV with a low-threshold 4π detection system. We have examined the multifragment decays of the system as a function of the multiplicity of charged particles. In collisions with more than 35 emitted charged particles, an average number of $\langle N_{IMF}\rangle \geq 6$ intermediate mass fragments was detected, and events with $N_{IMF}=14$ were observed. For such central collisions, intermediate mass fragments constitute 16-17% of all detected charged particles. Statistical models, based on the decay of nuclear systems at normal density, produce many fewer fragments

than observed. Similarly small fragment multiplicities are predicted by the quasi-particle dynamics model of ref. [8]. The observed relation between charged particle and intermediate mass fragment multiplicities can be roughly reproduced by calculations of the evaporative decay of an expanding nuclear system characterized by a soft equation of state at low density.

We gratefully acknowledge fruitful discussions with Professor D.H. Boal and his permission to use the QPD program of ref. [8]. This work is based upon work supported by the National Science Foundation under Grant numbers PHY-86-11210, PHY-89-13815, PHY-90-15255, and the U.S. Department of Energy under Contract No. DE-AC03-76SF00098. W.G. Lynch acknowledges the receipt a of U.S. Presidential Young Investigator Award and N. Carlin acknowledges partial support by the FAPESP, Brazil.

References

† Present address: Instituto de Física, Universidade de São Paulo, C. Postal 20516, CEP 01498, São Paulo, Brazil

1. W. Lynch, Ann. Rev. Nucl. Part. Sci., 37, 493 (1987).
2. D.H.E. Gross, Rep. Prog. Phys. 53, 605 (1990).
3. L.G. Moretto, Nucl. Phys. A247, 211 (1975).
4. W.A. Friedman and W.G. Lynch, Phys. Rev. C28, 16 (1983); C28, 950 (1983).
5. W.A. Friedman, Phys. Rev. C42, 667 (1990).
6. W. Bauer et al., Phys. Rev. Lett. 58, 863 (1987).
7. G. Peilert et al., Phys. Rev. C39, 1402 (1989).
8. D.H. Boal and J.N. Glosli, Phys. Rev. C37, 91 (1988); C42, R502 (1990).
9. H. Lamb, "Hydrodynamics", Dover Publications, New York (1945).
10. G. Bertsch and P.J. Siemens, Phys. Lett. 126B, 9 (1983).
11. L.P. Cernai and J. Kapusta, Phys. Reports 131, 223 (1986).
12. T.J. Schlagel, and V.R. Pandharipande, Phys. Rev. C36, 162 (1987).
13. K.G.R. Doss et al., Phys. Rev. Lett. 59, 2720 (1987).
14. R. Bougault, et al., Nucl. Phys. A488, 255c (1988).
15. R. Trockel et al., Phys. Rev. C39, 729 (1989).
16. R. Bougault et al., Phys. Lett. B232, 291 (1989).
17. Y.D. Kim et al., Phys. Rev. Lett. 63, 494 (1989).
18. Y. Blumenfeld et al., Phys. Rev. Lett. 66, 576 (1991).
19. R.T. de Souza et al., Nucl. Instr. and Meth. A295, 109 (1990).
20. J.T. Walton et al., IEEE Trans. Nucl. Sci. 37, 1578 (1990).
21. C. Cavata et al., Phys. Rev. C42, 1760 (1990).
22. The most forward ring of the hodoscope was excluded to reduce contributions from quasielastic reactions.

23. E. Piasecki et al., Phys. Rev. Lett. 66, 1291 (1991).

24. For central collisions, complete overlap of projectile and target occurs at t≈50 fm/c.

25. R.J. Charity et al., Nucl. Phys. A483, 371 (1988).

26. In its present formulation, GEMINI does not incorporate a temperature dependence of the conditional barriers. While a consistent treatment of such a temperature dependence is not yet available, preliminary calculations indicate that a reduction of the conditional barriers at higher temperatures can lead to fragment multiplicities comparable to those observed experimentally.

Figure Captions

Fig. 1: Upper panel: Measured charged particle multiplicity distribution, N_C, for the $^{129}Xe+^{197}Au$ reaction at E/A=50 MeV. Lower panel: Measured IMF multiplicity distributions, N_{IMF}, for the indicated gates on N_C. All distributions have been normalized to unit area.

Fig. 2: Summed charge of particles detected at $\theta_{lab} \approx 5.6°-160°$ for various gates on charged particle multiplicity.

Fig. 3: Relation between average IMF and charged particle multiplicities. Solid points represent measured values. Curves, crosses and open circular points represent calculations discussed in the text. Diamond and star-shaped points illustrate instrumental distortions: open diamonds represent assumed primary distributions, and star shaped points depict corresponding values filtered by the response of the experimental apparatus.

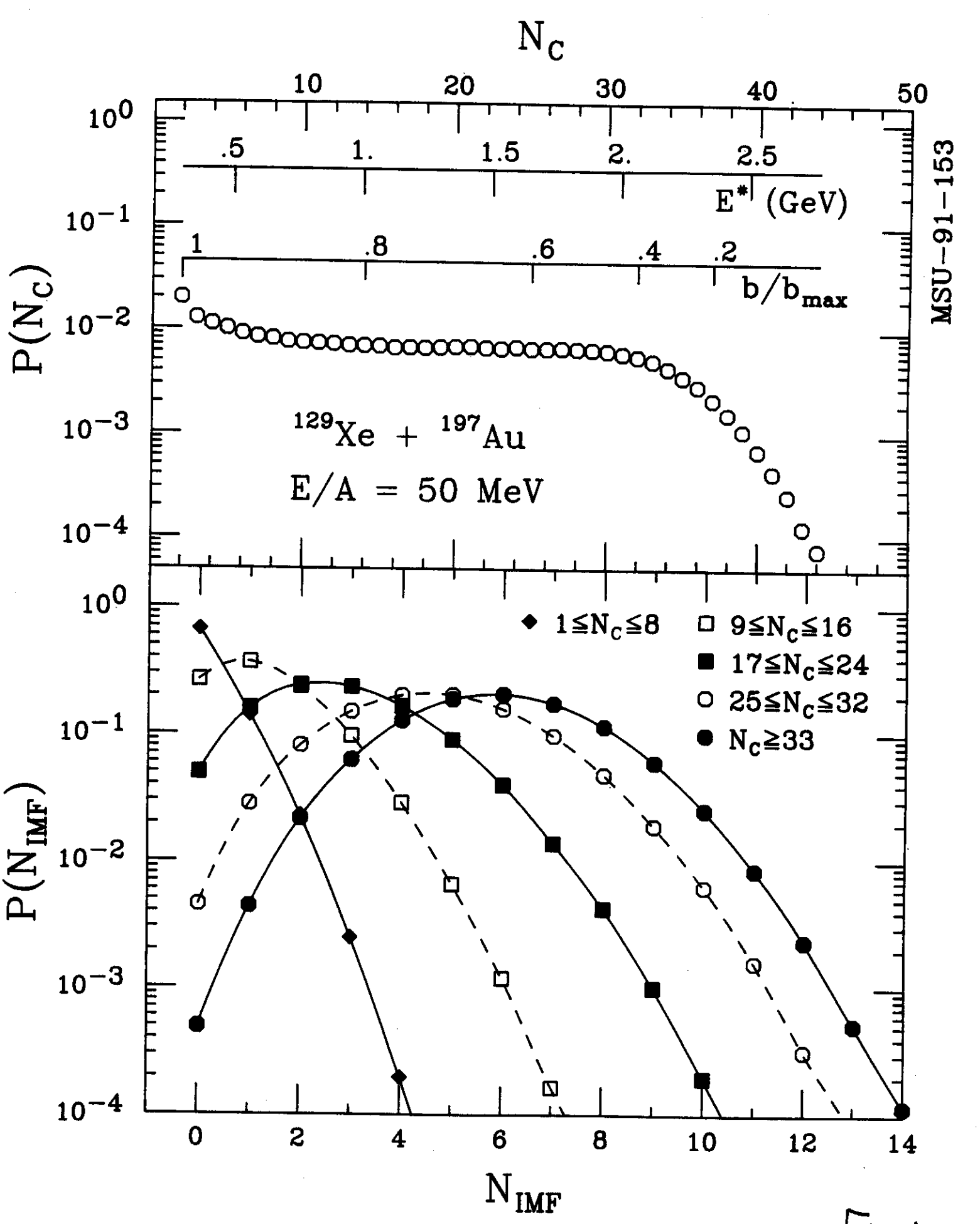
N_C
10
20
30
40
50
10^0
10^-1
10^-2
10^-3
10^-4
.5
1.
1.5
2.
2.5
E* (GeV)
1
.8
.6
.4
.2
b/b_max
P(N_C)
129Xe + 197Au
E/A = 50 MeV
MSU-91-153
1≦N_C≦8
9≦N_C≦16
17≦N_C≦24
25≦N_C≦32
N_C≧33
P(N_IMF)
0
2
4
6
8
10
12
14
N_IMF

Fig. 1

$^{129}Xe + ^{197}Au$, E/A = 50 MeV
$1 \leq N_c \leq 8$
$9 \leq N_c \leq 16$
$17 \leq N_c \leq 24$
$25 \leq N_c \leq 32$
$N_c \geq 33$
$P(Z_{sum})$
Z_{sum}
10^{-1}
10^{-2}
10^{-3}
10^{-4}
0
25
50
75
100
125

Fig. 2

MSU-91-155

Fig. 3